Bose-Einstein condensation in liquid ^{4}He under pressure

H. R. Glyde, S. O. Diallo, R. T. Azuah, O. Kirichek, and J. W. Taylor

Phys. Rev. B **83**, 100507 — Published 14 March 2011

DOI: 10.1103/PhysRevB.83.100507

Bose-Einstein condensation in liquid ^{4}He under pressure

H.R. Glyde,[1] S.O. Diallo,[2] R.T. Azuah,[3,4] O. Kirichek,[5] and J.W. Taylor[5]

[1]*Department of Physics and Astronomy, University of Delaware, Newark, Delaware 19716-2593, USA*
[2]*Spallation Neutron Source, Oak Ridge National Laboratory, Oak Ridge, TN 37831, USA*
[3]*NIST Center for Neutron Research, Gaithersburg, Maryland 20899-8562, USA*
[4]*Department of Materials Science and Engineering, University of Maryland, College Park, Maryland 20742-2115, USA*
[5]*ISIS Spallation Neutron Source, STFC, Rutherford Appleton Laboratory, Didcot, OX11 0QX, United Kingdom*

(Dated: February 24, 2011)

We present neutron scattering measurements of Bose-Einstein condensation, the atomic momentum distribution and Final State effects in liquid ^{4}He under pressure. The condensate fraction at low temperature is found to decrease from $n_0 = 7.25 \pm 0.75\%$ at SVP ($p \simeq 0$) to $n_0 = 3.2 \pm 0.75\%$ at pressure $p = 24$ bar. This indicates an $n_0 = 3.0\%$ in the liquid at the liquid/solid co-existence line ($p = 25.3$ bar). The atomic momentum distribution $n(\mathbf{k})$ has high occupation of low k states and differs significantly from a Gaussian (e.g. a classical $n(\mathbf{k})$). Both $n(\mathbf{k})$ and the Final state function broaden with increasing pressure, reflecting the increased localization of the ^{4}He in space under increased pressure.

PACS numbers: 61.05.fg,67.10.Ba,67.25.D−

In 1924 Bose[1] proposed Bose-Einstein quantum statistics and immediately thereafter Einstein[2] proposed Bose-Einstein condensation (BEC). In BEC, a macroscopic fraction of a system of Bosons condenses into one single particle state. In 1938, London[3] proposed that BEC was the origin of superfluiditiy in liquid ^{4}He, an observable manifestation of BEC in nature. In today's language, the superfluid velocity in a uniform Bose fluid is given by $v_s = -(\hbar/m) \bigtriangledown \phi$ where ϕ is the phase of the macroscopically occupied single particle state, $\psi = \sqrt{n_0} \exp[i\phi]$. Today, BEC can be observed directly in neutron scattering measurements.[4–9]. In bulk liquid ^{4}He at saturated vapor pressure (SVP) (p$\simeq$ 0), a fraction[9] $n_0 = 7.25 \pm 0.75\%$ condenses into the zero momentum (k = 0) state at low temperature.

In 1995, BEC was spectacularly observed in dilute gases of alkali atoms confined in traps[10–12]. In these dilute gases, essentially 100 % of the gas can condense into a single particle state. The superfluid velocity is again given by the expression above but the state ψ now depends on the shape of the potential confining the gas. As density is increased, the Bosons in a fluid become confined in configuration space by their neighbors. Since confinement in both configuration and momentum space is not possible, all Bosons cannot be confined in the zero momentum state and n_0 decreases dramatically with increasing density[13] dropping to the value noted above in liquid ^{4}He at SVP (density, $\rho = 0.146$ gm/cm^3). Recently, an apparent superfluid fraction in solid helium has been reported[14]. While this report is confirmed in independent measurements, the superfluid fraction observed varies greatly from measurement to measurement and superflow appears to be associated with defects[15–17]. Apparently conflicting properties[18–20] are also reported. Observation of BEC in solid ^{4}He, whether associated with defects or not, would be an unambiguous verification of superflow. However, BEC has not yet been observed[21].

In this context we present precision measurements of the condensate fraction, n_0, in liquid ^{4}He as a function of pressure, from SVP up to the solidification pressure, p = 25.3 bar. The goal is to determine n_0 at higher density with the same precision as it is known at SVP. Of special interest is the condensate fraction in the liquid at the liquid/solid interface. We also determine the density dependence of the atomic momentum distribution, $n(\mathbf{k})$, and the Final State (FS) function. We find that n_0 decreases from $n_0 = 7.25 \pm 0.75\%$ at SVP (p $\simeq$ 0) to $n_0 = 3.2 \pm 0.75\%$ at p = 24 bar. Comparison with Monte Carlo calculations[22,23] shows good agreement. From this density dependence an n_0= 3 % in the liquid at the liquid/solid interface is expected. Both $n(\mathbf{k})$ and the FS function broaden with increasing density. Commercial grade ^{4}He (0.3 ppm of ^{3}He) was liquified in a cylindrical aluminum sample cell of volume 100 cm^3 at the pressures and to the temperatures reported below. The neutron scattering measurements were carried out on the MARI time of flight (TOF) spectrometer at the ISIS Facility, Rutherford Appleton Laboratory, UK. The incident neutron energy was 750 meV. The TOF data were converted to the dynamic structure factor (DSF) $J(Q, y)$ at constant wave vector transfer Q in the range $20 \leq$ Q ≤ 29 Å^{-1}. The energy transfer $\hbar\omega$ is expressed in the y variable, defined as $y = (\omega - \omega_R)/v_R$ where $\hbar\omega_R = (\hbar\mathbf{Q})^2/2m$ and $v_R = \hbar\mathbf{Q}/m$ are the free atom recoil energy and velocity, respectively. In these units $J(Q, y)$ is the atomic momentum distribution modified by Final State effects.

Fig. 1 shows the observed $J(Q, y)$ at wave vector transfer Q = 27.5 Å^{-1} versus y of liquid ^{4}He in the Bose condensed and in the normal liquid phases. At 12 and 24 bar the superfluid to normal liquid transition is at $T_\lambda = 2.03$ and 1.86 K, respectively. The condensate contributes to $J(Q, y)$ chiefly at $y = 0$. The $J(Q, y)$ is larger at low temperature than in the normal phase at $y \simeq 0$ reflect-

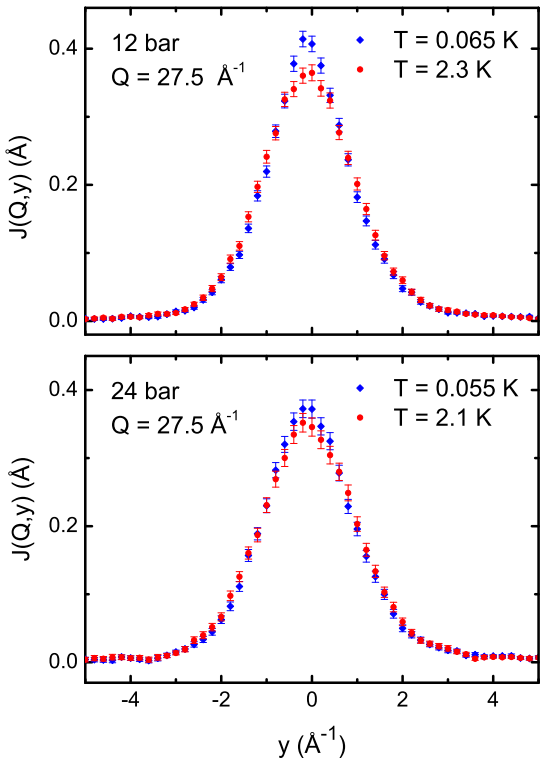

FIG. 1: (Color online) Observed dynamic structure factor of liquid ^{4}He, $J(Q,y)$, at wave vector Q = 27.5 Å folded with the instrument resolution. Shown is $J(Q,y)$ versus y, the energy transfer in momentum units, at low temperature in the Bose condensed phase (blue diamonds) and in the normal liquid phase (red circles) at pressures p = 12 and 24 bar. The difference between $J(Q,y)$ at $y \simeq 0$ in the Bose condensed and normal liquid phases, which arises chiefly from BEC, clearly decreases with increasing pressure.

ing the condensate contribution. This difference clearly decreases in magnitude with increasing pressure.

To interpret the data in Fig. 1, we introduce a model atomic momentum distribution,

$$n(\mathbf{k}) = n_0[\delta(\mathbf{k}) + f(\mathbf{k})] + A_1 n^*(\mathbf{k}), \qquad (1)$$

where n_0 is the condensate fraction, $n^*(\mathbf{k})$ is the momentum distribution over the $k \geq 0$ states and f($\mathbf{k}$) is a small term arising from the coupling of single particle and density excitations via the condensate. The f($\mathbf{k}$) is derived and discussed in Ref [25] and including it reduces n_0 by 15 %. A_1 is a normalization constant. The one body density matrix (OBDM) $n(\mathbf{r})$ is the Fourier transform of $n(\mathbf{k})$. The model OBDM, $n(s)$, corresponding to Eq. (1) for displacements $\mathbf{r} = \widehat{\mathbf{Q}}\, s$ parallel to wave vector $\mathbf{Q}$ is,

$$J_{IA}(s) = n(s) = n_0[1 + f(s)] + A_1 n^*(s). \qquad (2)$$

The intermediate DSF in the Impulse Approximation (IA), $J_{IA}(s)$, is this OBDM. The OBDM in Eq. (2) is our

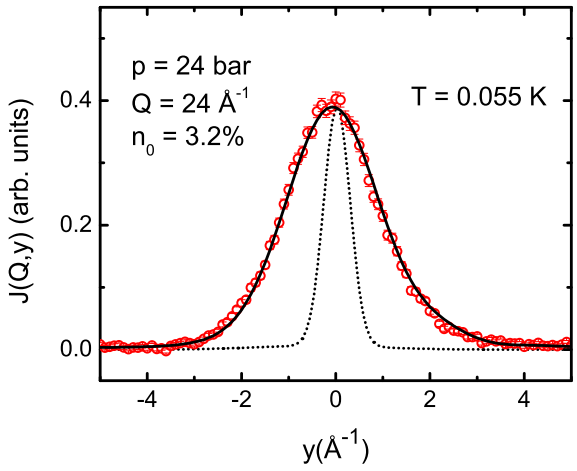

FIG. 2: (Color online) Observed $J(Q,y)$ (open circles) at pressure p = 24 bar and temperature T = 0.055 K showing a fit (solid line) of the model $J(Q,y)$ given by Eq. (3) to the data. Both the observed and fitted $J(Q,y)$ include the MARI instrument resolution function shown by the dotted line. A condensate fraction, n_0 = 3.2 %, provides the best fit.

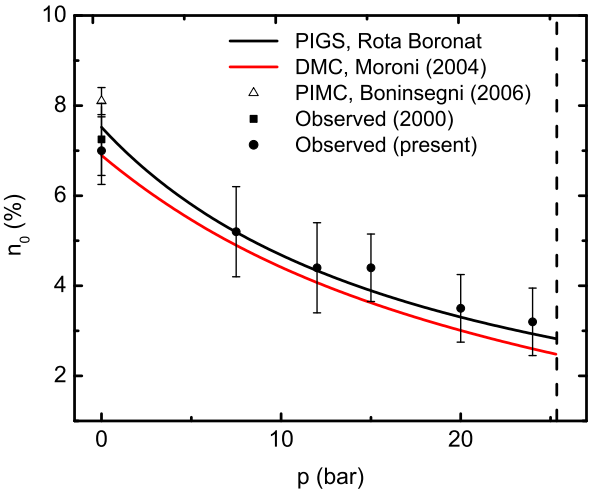

FIG. 3: (Color online) Condensate fraction, n_0, at low temperature in liquid ^{4}He versus pressure. The solid circles are the present observed values. The lines are calculated values, PIGS by Rota and Boronat[22] and DMC by Moroni and Boninsegni.[23] At SVP, values calculated by Boninsegni et al.[24] (triangle) and observed previously[9] are also shown.

basic model. The observed DSF $J(Q,s)$ is $J(Q,s) = J_{IA}(s)R(Q,s)$ which may be taken as the definition of the FS function $R(Q,s)$. In the y variable, the observed DSF shown in Fig.1 is the Fourier transform of $J(Q,s)$,

$$J(Q,y) = \frac{1}{2\pi}\int ds\; e^{iys} J_{IA}(s) R(Q,s). \qquad (3)$$

An expansion of $J(Q,s)$ in powers of s provides a

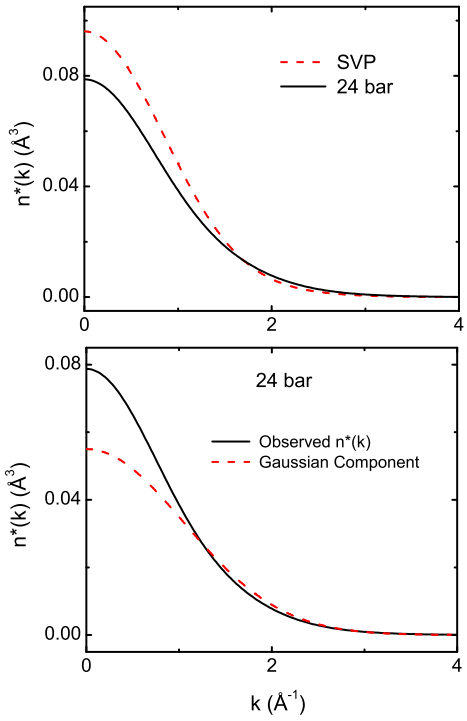

FIG. 4: (Color online) Top: The 3D momentum distribution $n^*(\mathbf{k})$ for the liquid above the condensate at SVP and 24 bar. Bottom: The 3D $n^*(\mathbf{k})$ at 24 bar and its Gaussian component ($\overline{\alpha}_4 = \overline{\alpha}_6 = 0$).

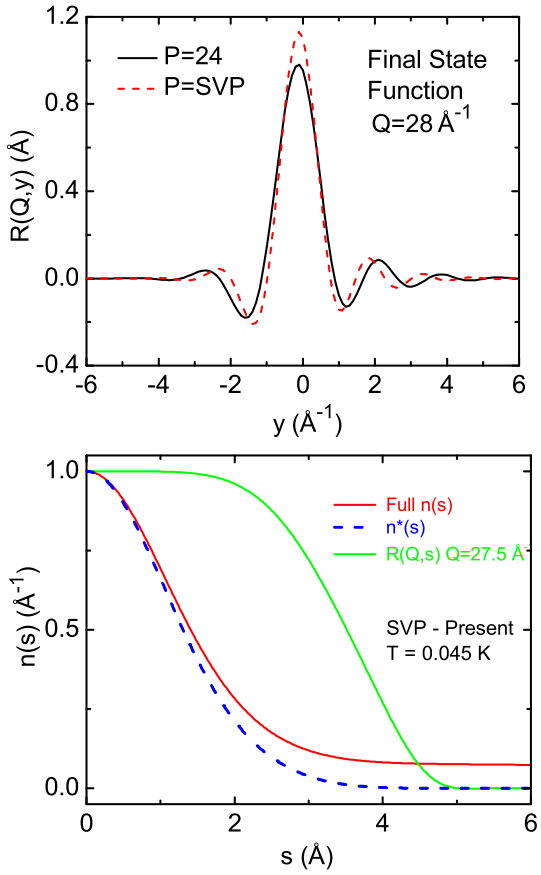

FIG. 5: (Color online) Top: The Final State (FS) function $R(Q,y)$ at SVP and 24 bar. $R(Q,y)$ broadens with increasing pressure. Bottom: The One body density matrix (OBDM) of the Bose condensed liquid, $n(s)$, given by Eq. (2), and $n^*(s)$ at SVP. Also shown is the FS function $R(Q,s)$ at $Q = 27.5$ Å.

model for $n^*(s)$ and $R(Q,s)$. The model $n^*(s)$ is,

$$n^*(s) = \exp\left[-\frac{\bar{\alpha}_2 s^2}{2!} + \frac{\bar{\alpha}_4 s^4}{4!} - \frac{\bar{\alpha}_6 s^6}{6!}\right], \qquad (4)$$

a Gaussian plus corrections where the $\bar{\alpha}_n$ are cumulants of the momentum distribution.

Fig. 2 shows a fit of the model $J(Q,y)$ given by Eqs. (3), (2) and (4) to the data at 24 bar. The fit is obtained by treating the parameters n_0, $\overline{\alpha}_2$, $\overline{\alpha}_4$ and $\overline{\alpha}_6$ and parameters in the model $R(Q,s)$ as free parameters[9] to be determined by least squares fit to data. In a single fit to a given $J(Q,y)$, 3-4 parameters can be determined uniquely. The $n^*(s)$ and $R(Q,s)$ were found to be reasonably independent. Given the large amount of data ($J(Q,y)$ at 10 - 12 Q values at each pressure and temperature), values for seven parameters could be obtained as a function of pressure with reasonable precision. A fit obtained for $n_0 = 3.2$ % is shown in Fig. 2.

Fig. 3 shows the best fit condensate fraction versus pressure, the central result of the present paper. The n_0 calculated using diffusion Monte Carlo (DMC) and path intergral ground state Monte Carlo (PIGS) methods[22,23] shown in Fig. 3 clearly agree well with experiment. The reader is referred to Refs. 22,23 for a discussion of calculated errors. Taken together, the present observed and recent Monte Carlo calculations provide accurate values of n_0.

The upper half of Fig. 4 shows the atomic momentum distribution $n^*(\mathbf{k})$ of the fluid for $\mathbf{k}$ states above the condensate, the Fourier transform of $n^*(s)$ given by Eq. (4). The $n^*(\mathbf{k})$ clearly broadens with increasing pressure. The $n^*(\mathbf{k})$ broadens under pressure because the ^{4}He atoms are more localized in space under pressure. The lower half of Fig. 4 compares the full $n^*(\mathbf{k})$ with its Gaussian component, obtained by setting $\overline{\alpha}_4$ and $\overline{\alpha}_6$ to zero in Eq. (4). The full $n^*(\mathbf{k})$ has much higher occupation of low momentum states than a Gaussian $n(\mathbf{k})$, as might be expected in a cold quantum liquid,

The upper half of Fig. 5 shows the Final State (FS) broadening function $R(Q,y)$. The R(Q,y) also broadens with increasing pressure reflecting the increased interaction of the struck atom with its neighbors at higher density. In the IA where FS effects are neglected, $R(Q,y)$ reduces to a delta function, $\delta(y)$. The lower half of Fig. 5 shows the corresponding $R(Q,s)$ at SVP. The $R(Q,s)$ takes a simple form decreasing uniformly with increasing s from $R(Q,s) = 1$ at $s = 0$ to zero at $s \simeq 4.4$

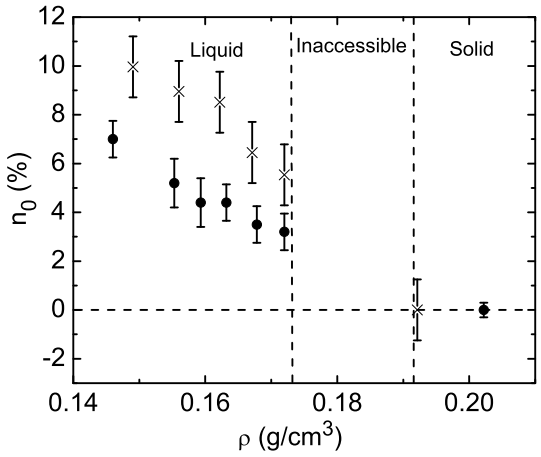

FIG. 6: Condensate fraction, n_0, at low temperature versus density. Solid circles are present values and that of Diallo et al.[21]and the crosses are earlier values observed by Snow et al[8].

Å. Also shown in Fig. 5 is the OBDM $n(s)$ including the flat long range component (ODLRO) arising from BEC. The chief impact of the FS $R(Q,s)$ in the observed product $J(Q,s)= R(Q,s)n(s)$ is to cut off $J(Q,s)$ at $s \simeq 4.4$ Å so that the ODLRO in $n(s)$ can be observed in $J(Q,s)$ over a limited range of s only. In the IA, $R(Q,s) = 1$ for all values of s.

Finally, Fig. 6 shows the observed condensate fraction, n_0, versus density observed in liquid and solid ^{4}He. The present values in the liquid and those in the solid observed by Diallo et al.[21] are shown as well as the earlier liquid and solid data of Snow et al.[8] In the liquid, the present values lie significantly below previous observed values. From Figs. 3 and 6, the present observed value of n_0 in the liquid at the solid/liquid interface ($p = 25.3$ bar, $\rho = 0.172$ gm/cm^3) is $n_0 = 3.0\%$. The values observed in crystalline solid ^{4}He shown in Fig. 6 are zero within the error shown. Current predictions of n_0 in the solid are zero for perfect crystalline solids[26–28] and 0.5 % for amorphous solids.[28] In solids containing vacancies, predictions are $n_0= 0.23$ % for a vacancy concentration $c_V = 1$ % at pressure $p = 54$ bars[29] and $n_0= 0.09$ % at $c_V = 0.6$ % at $p \simeq 40$ bars[30]. The core of a dislocation is also predicted[31] to support BEC. Amorphous solid helium has a static structure factor similar to that of liquid helium[32]. Assuming that liquid and amorphous solid helium have similar condensate fractions, from Fig. 6 and on the basis of density alone, only a small n_0 is expected in amorphous solid helium at solid densities ($\rho \geq 0.19$ gm/cm^3) as is predicted[28] by PIMC..

In summary, we find that the condensate fraction, n_0, in liquid ^{4}He decreases significantly with increasing liquid density dropping to $n_0 = 3.0\%$ at the liquid/solid interface. The atomic momentum distribution $n(\mathbf{k})$ of liquid ^{4}He differs significantly from a Gaussian with large occupation of low k states. The kurtosis of the distribution is 0.40 independent of pressure. The $n(\mathbf{k})$ and the Final State function both broaden with increasing pressure.

We thank Richard Down for valuable technical assistance at ISIS and Jordi Boronat and Riccardo Rota for stimulating discussions. This work was supported by the U. S. DOE, Office of Science Grant No. DE-FG02-03ER46038.

[1] S. N. Bose, Z. Phys. **26**, 178 (1924).
[2] A. Einstein, Sitzungsber. Kgl. Preuss. Akad. Wiss. **261** (1924).
[3] F. London, Nature (London) **141**, 643 (1938).
[4] A. Miller, D. Pines, and P. Nozières, Phys. Rev. **127**, 1452 (1962).
[5] P. C. Hohenberg and P. M. Platzman, Phys. Rev. **152**, 198 (1966).
[6] V. F. Sears, E. C. Svensson, P. Martel, and A. D. B. Woods, Phys. Rev. Lett. **49**, 279 (1982).
[7] T. R. Sosnick, W. M. Snow, P. E. Sokol, and R. N. Silver, Europhys. Lett. **9**, 707 (1990).
[8] W. M. Snow, Y. Wang, and P. E. Sokol, Europhys. Lett. **19**, 403 (1992).
[9] H. R. Glyde, R. T. Azuah, and W. G. Stirling, Phys. Rev. B **62**, 14337 (2000).
[10] M. H. Anderson, J. R. Ensher, M. R. Matthews, C. E. Wieman, and E. A. Cornell, Science **269**, 198 (1995).
[11] K. B. Davis, M. O. Mewes, M. R. Andrews, N. J. van Druten, D. S. Durfee, D. M. Kurn, and W. Ketterle, Phys. Rev. Lett. **75**, 3969 (1995).
[12] C. C. Bradley, C. A. Sackett, J. J. Tollett, and R. G. Hulet, Phys. Rev. Lett. **75**, 1687 (1995), *ibid.* **79**, 1170 (1997).
[13] D.M. Ceperley, Rev. Mod. Phys. **67**, 279, (1995).
[14] E. Kim and M. H. W. Chan, Science **305**, 1941 (2004), Nature (London) **427**, 225 (2004).
[15] A. S. C. Rittner and J. D. Reppy, Phys. Rev. Lett. **101**, 155301 (2008).
[16] J. T. West, X. Lin, Z. G. Cheng, and M. H. W. Chan, Phys. Rev. Lett. **102**, 185302 (2009).
[17] S. Balibar, Nature (London) **464**, 176 (2010).
[18] J. D. Reppy, Phys. Rev. Lett. **104**, 255301 (2010).
[19] M. W. Ray and R. B. Hallock, Phys. Rev. Lett. **105**, 145301 (2010).
[20] H. Choi, D Takahashi, K. Kono, and E. Kim, Science **330**, 1512 (2010).
[21] S. O. Diallo, R. T. Azuah, O. Kirichek, J. W. Taylor, and H. R. Glyde, Phys. Rev. B **80**, 060504 (2009).
[22] R. Rota and J. Boronat, Phys. Rev. B submitted (2011).
[23] S. Moroni and M. Boninsegni, J. Low Temp. Phys. **136**, 129 (2004).
[24] M. Boninsegni, N. V. Prokof'ev, and B. V. Svistunov, Phys. Rev. E **74**, 036701 (2006).
[25] H. R. Glyde, *Excitations in Liquid and Solid Helium* (Oxford University Press, Oxford, England, 1994).
[26] D. M. Ceperley and B. Bernu, Phys. Rev. Lett. **93**, 155303 (2004).
[27] B. K. Clark and D. M. Ceperley, Phys. Rev. Lett. **96**, 105302 (2006).
[28] M. Boninsegni, N. V. Prokof'ev, and B. V. Svistunov, Phys. Rev. Lett. **96**, 070601 (2006).
[29] D. E. Galli and L. Reatto, Phys. Rev. Lett. **96**, 165301 (2006).
[30] R. Rota and J. Boronat, J. Low Temp. Phys. **162**, 146 (2011).
[31] L. Pollet, M. Boninsegni, A. B. Kuklov, N. V. Prokofev, B. V. Svistunov, and M. Troyer, Phys. Rev. Lett. **98**, 135301 (2007).
[32] J. Bossy, T. Hansen, and H. R. Glyde, Phys. Rev. B **81**, 184507 (2010).